Alexandria Engineering Journal (2016) 55, 2077–2086

Alexandria University

Alexandria Engineering Journal

www.elsevier.com/locate/aej
www.sciencedirect.com

ORIGINAL ARTICLE

Microstructure, consolidation and mechanical behaviour of Mg/n-TiC composite

N. Vijay Ponraj [a,*], **A. Azhagurajan** [b], **S.C. Vettivel** [c]

[a] *Department of Mechanical Engineering, PSN College of Engineering and Technology, Tirunelveli, Tamil Nadu, India*
[b] *Department of Mechanical Engineering, Mepco Schelenk Engineering College, Sivakasi, India*
[c] *Department of Mechanical Engineering, Chandigarh College of Engineering and Technology, Chandigarh, India*

Received 17 November 2015; revised 31 May 2016; accepted 25 June 2016
Available online 28 July 2016

KEYWORDS

Consolidation behaviour;
Magnesium;
Titanium carbide;
Compressibility;
Sinterability;
Compressive stress

Abstract In this work, the microstructure, consolidation and mechanical properties of pure magnesium, magnesium based composite containing with different fractions (5, 10, 15 wt%) of Titanium carbide nanoparticles (n-TiC) were fabricated via powder metallurgy technique. The fabricated composites exhibited homogeneous distribution of TiC with little porosity. Microstructure of the composite and powders was studied using X-ray diffraction, Scanning electron microscope, and Transmission electron microscope. Microstructural characterization of the materials exposed that the accumulation of nanosized titanium carbide reinforcement enhanced the homogenization during mechanical blending. The relative density, compressibility, green compressive strength, sinterability and hardness of the nanocomposites were also examined. The effect of reinforcement on the densification was studied and reported in terms of the relative density and consolidation behaviour of the Magnesium matrix with n-TiC was studied and best compacted fit obtained through the Heckel, Panelli Ambrosio Filho and Ge equations. The compressive strength of the composite significantly increases from 230 MPa to 389 MPa with content of n-TiC and sintering temperature. Experiments have been performed under different conditions of temperature, n-TiC Content, and compacting pressure.
© 2016 Faculty of Engineering, Alexandria University. Production and hosting by Elsevier B.V. This is an open access article under the CC BY-NC-ND license (http://creativecommons.org/licenses/by-nc-nd/4.0/).

1. Introduction

In the recent era there has been great interest in using magnesium (Mg) based materials in electronics, aerospace, medical applications due to its low density (1.74 g/cm^3) and high specific strength. Being one of the light weight metal among the structural materials and most abundant element in earth crust by 2.7 weight, magnesium based alloys have extend into a proficient part in areas where weight reduction is primary [1,2]. In the past decade research on magnesium composite as a "biomaterial" has exponentially increased [3]. Mg degrades naturally [4]. Young's modulus (40 GPa) is similar to that of human bone [5]. Since it is hexagonal close-packed (hcp) structure, strength is moderate and poor formability at room temperature [6]. Mg with reinforcement confirms strengthening

* Corresponding author.
E-mail addresses: vijayponrajmechauto@gmail.com (N.V. Ponraj), aazhagu@mepcoeng.ac.in (A. Azhagurajan), scvettivel@ccet.ac.in (S.C. Vettivel).
Peer review under responsibility of Faculty of Engineering, Alexandria University.

http://dx.doi.org/10.1016/j.aej.2016.06.033
1110-0168 © 2016 Faculty of Engineering, Alexandria University. Production and hosting by Elsevier B.V.
This is an open access article under the CC BY-NC-ND license (http://creativecommons.org/licenses/by-nc-nd/4.0/).

the mechanical properties [7]. Reinforcement such as ceramics, oxides and metals in nanoparticles with metal matrix shows better properties than microparticles [8]. Processing at low temperature, the undesired phases between the matrix phase and the reinforcement are prevented due to the reason hard ceramic reinforcements normally have a lot better physical and mechanical properties of the composite [9,10]. In previous studies it is shown that Mg nanocomposites enhance better mechanical properties and physical properties than magnesium micro composite [11]. Even various routes available for the synthesis of Mg composites, fine grained composites with near-uniform distribution, highest promising reinforcement content can be produced via powder metallurgy route [12]. In addition due to simplicity, flexibility, low processing cost and high production rate for synthesizing discontinuously reinforced composites make highly preferable [13]. On consideration of nano level attempt P/M is the promising one, the mechanical properties of Mg are improved by dispersing hard and stable particles of nano-TiC a face centred cubic (fcc) structure [14]. Nano TiC is used as reinforcement in magnesium matrices due to its desirable characteristics such as low densities (4.93 g/cm^3), high melting point (3067 °C), good thermal and chemical stability, high Young's modulus (300–480 GPa), high hardness (28–35 GPa), excellent wear resistance [15,16] and good wettability [17]. TiC have strong interface [18]. No sign of toxicity was observed while dosing TiC in rats [19]. Since n-Tic possess high mechanical properties with non-toxic character makes it as potential reinforcement in mg metal for manufacturing bio components and materials.

The addition of nanoparticles significantly varies with the compaction behaviour of the matrix powder [20]. The consolidation behaviour of the Mg composites was evaluated by using linear compaction equations, such as the Balshin [21], Heckel [22], Panelli and Ambrozio Filho [23] and Ge [24] equations.

Balshin equation:

$$\frac{1}{D} = K \ln P + B$$

Heckel equation:

$$\ln\left(\frac{1}{1-D}\right) = KP + B$$

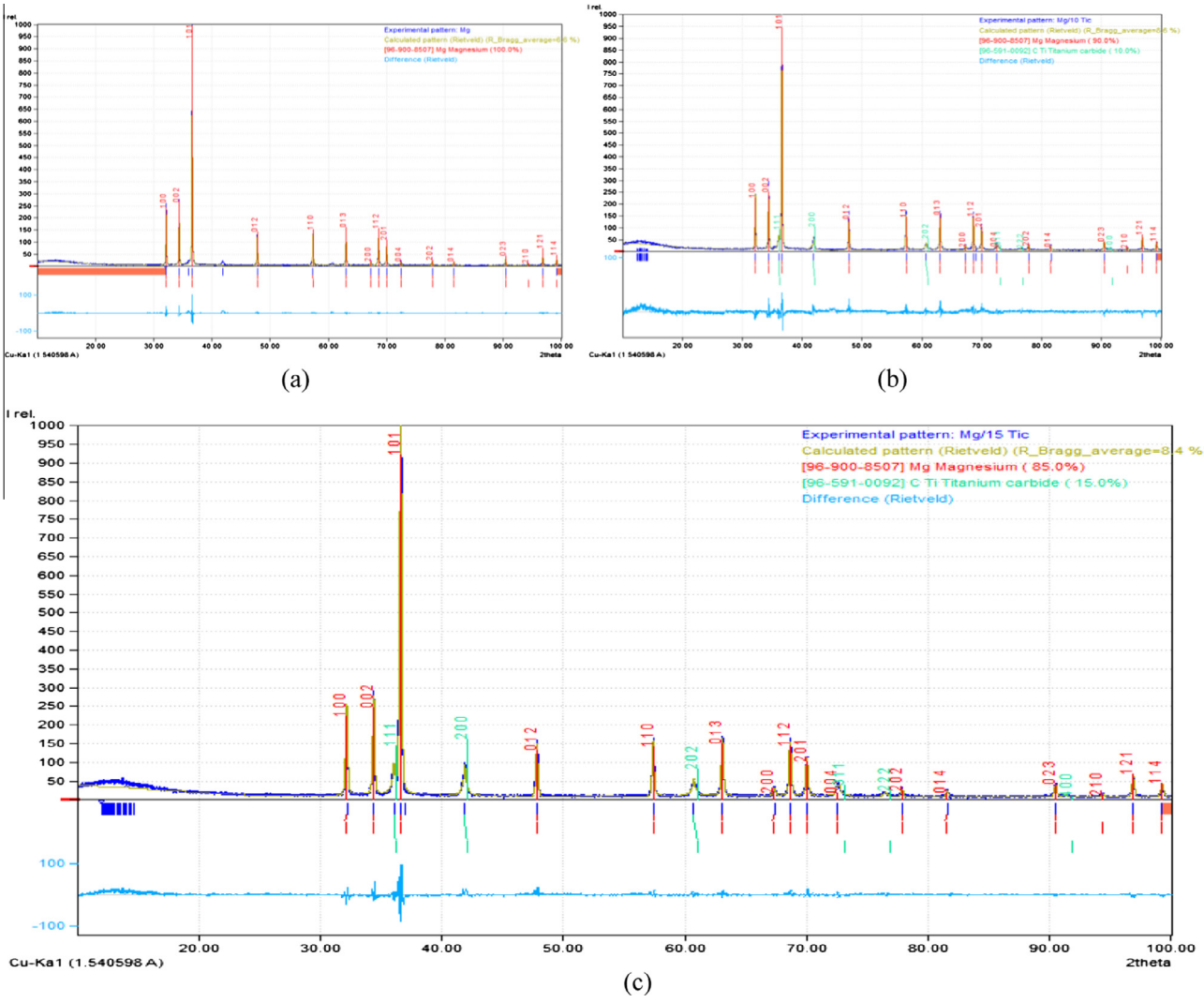

Figure 1 (a–c) shows the XRD results of the prepared Mg, Mg/10TiC, and Mg/15 TiC.

Panelli and Ambrozio Filho equation:

$$\ln\left(\frac{1}{1-D}\right) = K\sqrt{P} + B$$

Ge equation:

$$\log\left(\ln\left(\frac{1}{1-D}\right)\right) = K\log P + B$$

where D is the relative density of compacted material and P is the applied pressure. K and B are fitting parameters. The parameter 'K' is related to the plastic deformation ability of the powder particles throughout the compacting process. The parameter 'B' articulates the density exclusive of applied pressure, which is the apparent density. The above linear compaction equations contribute to the improvement of revising the position of plastic deformation on the densification rate of composite powders. The link between the compacting pressure and the density of the green compact was appraised based on the density-compaction pressure curve [21–24]. The parameter 'A' (also called densification index) is related to the plastic deformation capacity of the powder during compacting process. High 'A' values are obtained when the soft metals such as Magnesium or copper are used and low 'A' values are for hard powders, such as ceramics. The parameter 'B' expresses the density without applied pressure, which is the apparent density [25,26]. The role of hard n-TiC particles in the compacting process was also investigated. Furthermore, the compressibility curves were plotted and examined using the Balshin, Heckel, Panelli and Ambrosio Filho and Ge equations. Then, the sinterability of the nanocomposites was investigated at different sintering temperatures. The effects of the sintering temperature of each nanocomposite on the density, sinterability and compressive stress of the sintered composites were also investigated.

Previously, Hwang et al. [27] studied the compressive properties of Mg 15 vol% TiC (6 nm) nanocomposite fabricated by ball milling. For synthesizing Mg/n-TiC nanocomposites, pure Mg (99.6% pure, ~325 mesh), Ti (99.98%, ~325 mesh) and C (99.5%) powders were mechanically milled for 24 h in an Argon atmosphere. Ball to powder charge ratio was 10:1. These milled powders were pressed and then sintered at 350 °C for 1 h in vacuum condition. The nanocomposite shows evidence of high compression properties and also possesses high strength 320 Mpa. The compressive fracture strain is of 28%. After heat treatment at 350 °C for 1 h, the compression strength of the nanocomposites was improved by 8% (345 MPa) with decrease in compressive fractures strain (to 15%). Jeyasimman et al. [28] investigated the consolidation behaviour of Tic reinforcement with Al 6061 matrix. The compressibility curves of the developed composite powders were also plotted and investigated using the Heckel, Panelli and Ambrosio Filho and Ge equations. Due to addition of TiC shows good compressibility with decrease in densification rate. Theoretical density increased with the size reduction of TiC.

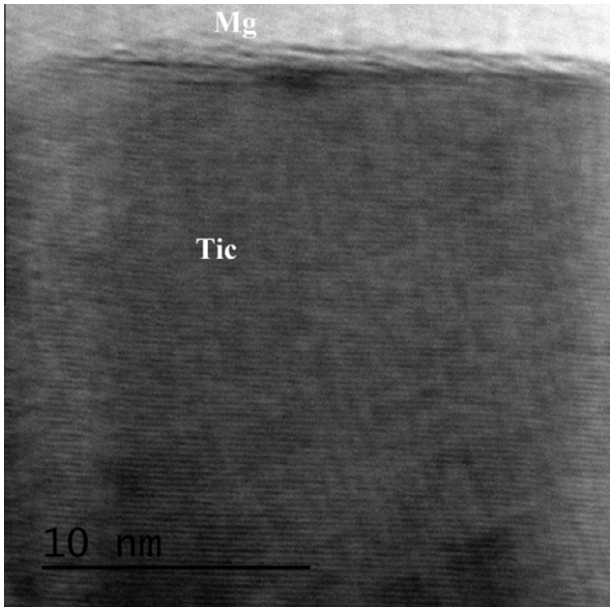

Figure 2 TEM Microstructure of interface between TiC and Mg particles.

Accordingly in this study, Mg with different wt% of n-TiC reinforced nanocomposites is synthesized by the powder metallurgy technique and also the mechanical, consolidation behaviour and microstructural characteristics of the nanocomposites were studied. To the best of author knowledge no work has been done on consolidation behaviour with Mg/nano TiC composite.

2. Materials and methods

2.1. Materials

In this study, pure magnesium (99.9% purity, ~30 μm) and Titanium Carbide (99.5% purity, ~200 nm) are brought from Sigma-Aldrich.

2.2. Synthesis, characterization and experiment

In this investigation, Mg powder and TiC nanosized powders were used to produce Mg/n-TiC composite. The Mg and TiC mixture was cold compacted in a steel die using uniaxial hydraulic press at a pressure ranging from 300 to 500 MPa. The die walls were lubricated by applying a small quantity of graphite powder. These given compacts were well covered with fine alumina powder to prevent oxidation during sintering process. The sintering process was carried out in an electric muffle furnace at the temperature of 350, 400 and 450 °C for 1 h in argon atmosphere. The sintered density (ρ) was measured using Archimedes' principle. The weights of the sintered specimens in air and water were measured with the help of an electronic balance (Denver) with an accuracy of ±0.01 mg. The micro structure and phase analysis of the compacted composites were examined using Scanning Electron Microscope (SEM) (Carl Zeiss EVO 18) with EDX mapping, Transmission electron Microscope (TEM) (Jeol/JEM 2100) and X-ray Diffraction (D8 Advance ECO XRD Systems with SSD160 1 D Detector).

2.2.1. X-ray diffraction analysis

In order to find the qualitative phase analysis X-ray powder diffraction (XRD) has been widely used since von Laue's discovery of the diffraction of X-rays in 1912 [29]. X-ray Diffraction (XRD) investigations of the prepared powder composites were carried out in X-ray Diffraction (D8 Advance ECO XRD

Systems with SSD160 1 D Detector). The XRD results of the prepared Mg, Mg/10TiC, Mg/15TiC are shown in Fig. 1(a)–(c). Peak values were collected over the 2θ range of 10–100° with a step size of 0.020 and step time of 48 s. All the samples showed wide diffraction peaks, which could be indexed to the structure of Mg. They exposed that the typical peaks in the XRD patterns which consistent standard pattern COD card No. 96-900-8507 for Mg, 96-591-0092 for TiC. In 1966, Rietveld suggested a method, known by his name as Rietveld method, where total pattern was fitted with a suitable function and decomposed it into individual Bragg reflections; moreover, subsequently structural modification was conceded out awaiting the best fit was achieved through the intact observed pattern The value of parameters analogous en route for the best fit furnishes the structure and some of the microstructural parameters of the system [30].

It is observed that intensity of n-TiC peaks increases with the increase in the percentage addition of n-TiC and

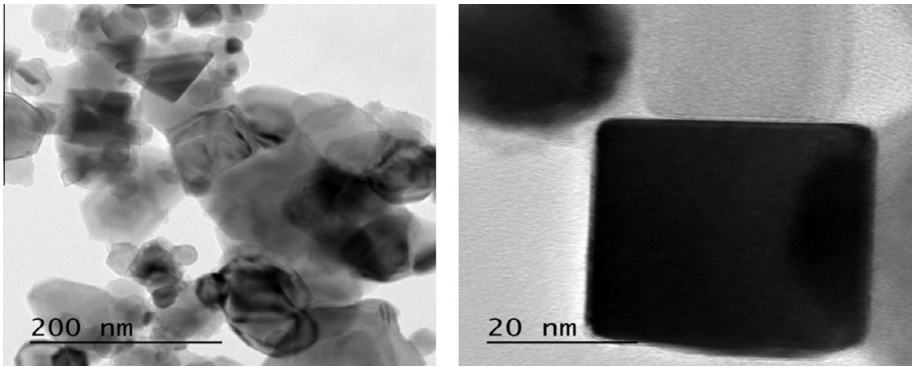

Figure 3 (a) TEM image of the composite shows the uniform distribution of TiC Composite and (b) TiC particles are separated by Mg.

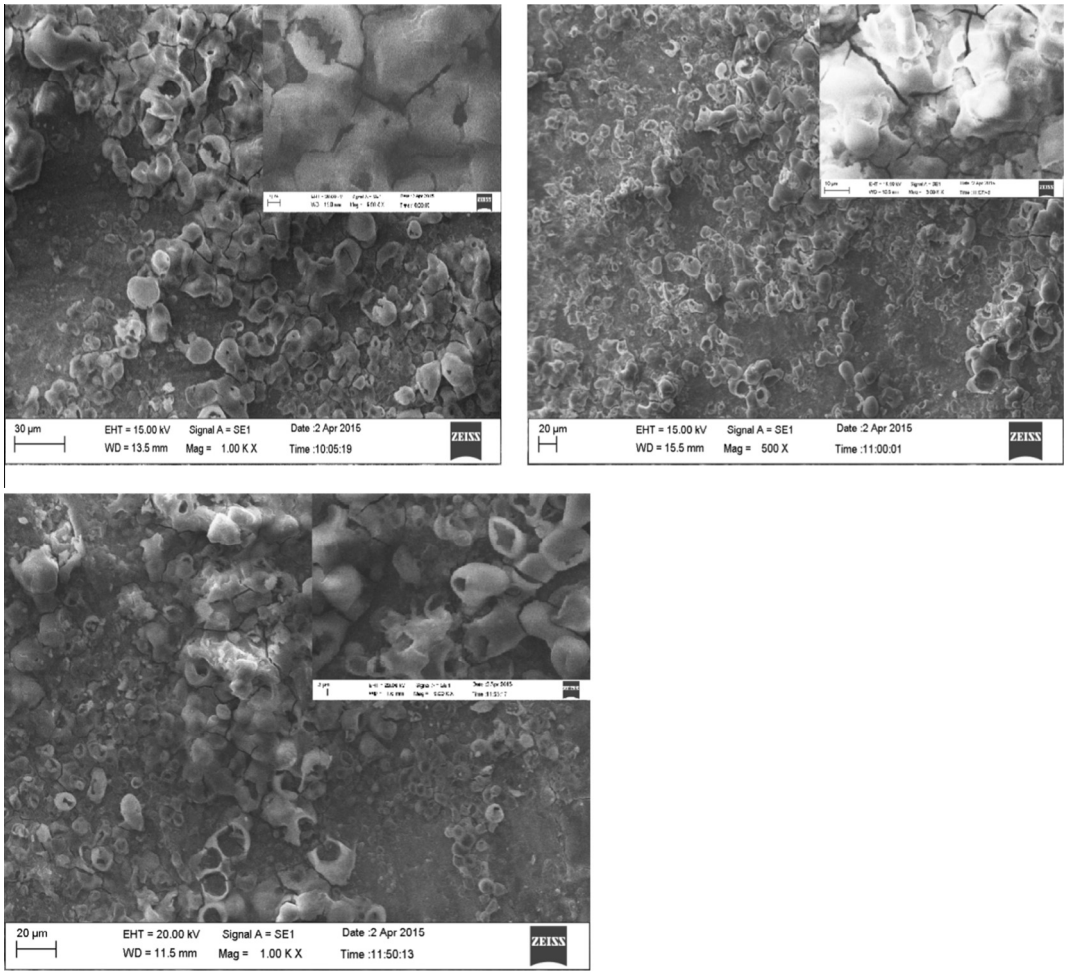

Figure 4 SEM image of (a) Mg/5TiC, (b) Mg/10TiC, (c) Mg/15TiC.

correspondingly the intensity of magnesium peaks decreases as the percentage of n-TiC addition increases. The XRD results reveal that the intensity of Mg was greater in the (101) plane (2θ = 36.61, COD card No. 96-900-8507). In addition, the intensity of Mg/n-TiC was observed at different peaks and definite through Match software, and the intensity for n-TiC is greater in (200) plane (2θ = 41.91, COD card No. 96-591-0092). The full pattern fitting of Rietveld method performed using FULLPROF program [31], R Bragg average = 8.4, 8.6 for Mg/n-15TiC, Mg/10 n-TiC is calculated. Fig. 1(b) and (c)

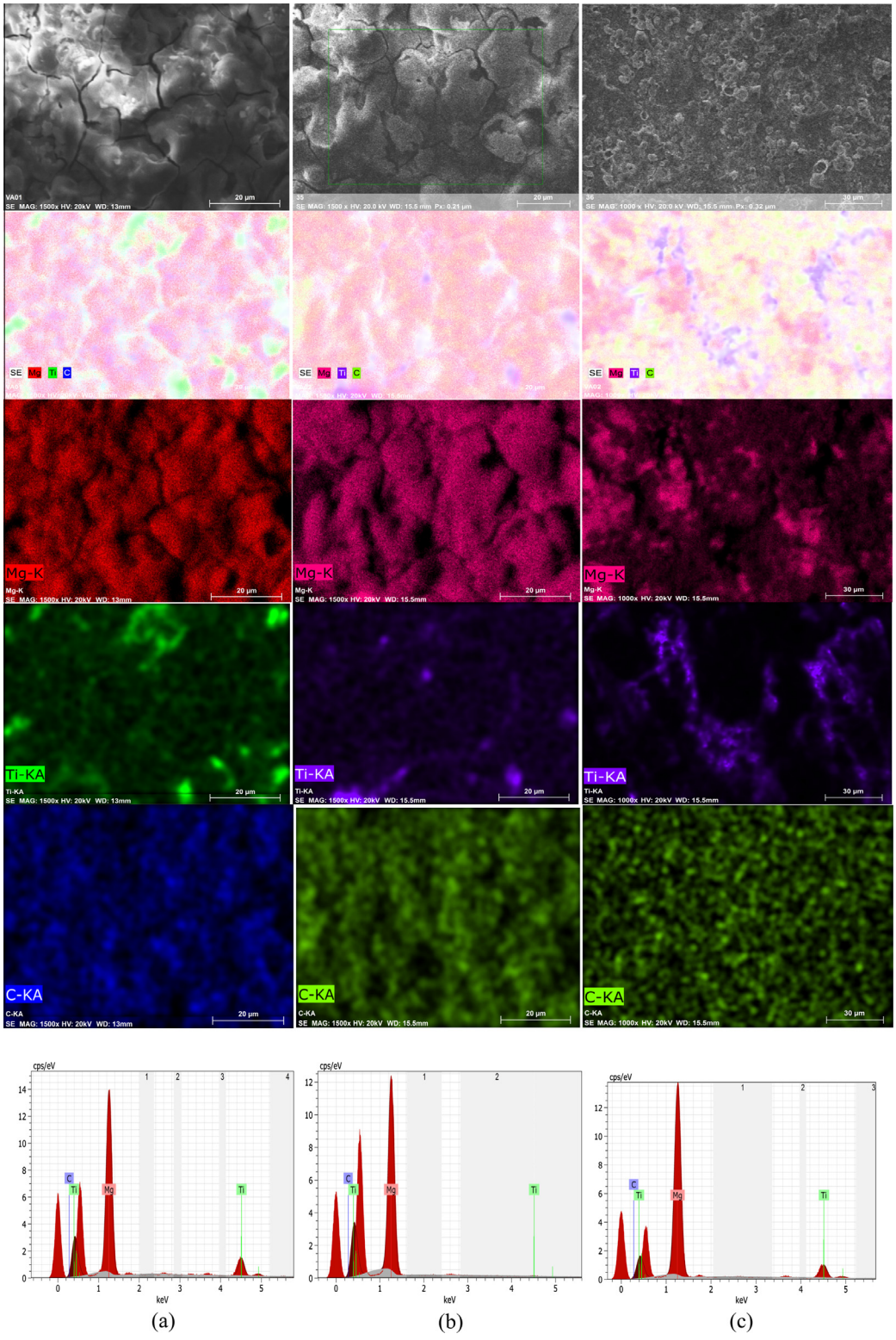

Figure 5 EDX Mapping of (a) Mg/5 TiC, (b) Mg/10 TiC, (c) Mg/15TiC.

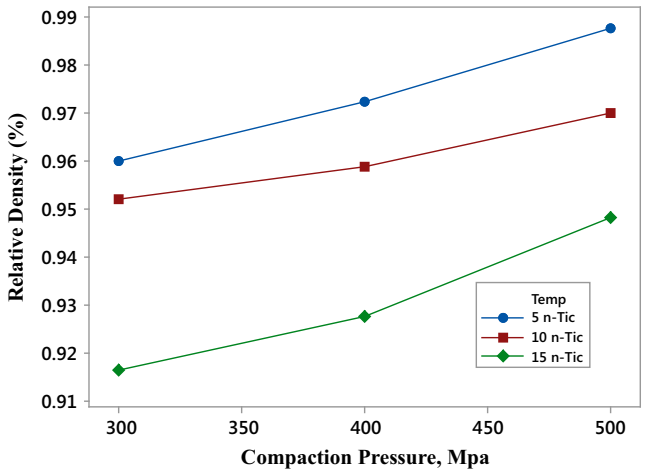

Figure 6 Compressibility curves.

shows the presence of Mg in large peaks notably at $2\theta = 32.19°$, 34.40°, 36.62°, 47.82°, 57.38°, 63.07°, 68.65°, 70.3° of (100), (002), (101), (012), (110), (013), (112) of the diffraction peak of Mg. The Presence of diffraction peak of TiC was indicated as minor peak notably at $2\theta = 36.07°$, 41.89°, 60.68°, 73.10°, 76.93° of (111), (200), (202), (311), (222). Fig. 1(b) & (c) shows, a gradual margin shift of mg peak to higher angles, with an increase in wt% of n-TiC. This points to that the structure remains the same even if the composition of composites is varied. All the peaks of the composites are identified. No other additional peak was observed apart from the parent material. This confirms the successful preparation of the two phase composite material.

3. Microstructural characterization

In order to characterize the microstructure of Mg/n-TiC composite, the TEM, SEM, and EDX mapping are used. The interface of Mg and TiC is examined through the Transmission Electron microscopy (TEM). TEM image reveals the presence of very small amount of equiaxed n-TiC which is shown in Fig. 2. It is noted that the components are strongly connected and precipitate free interference obtained.

In Fig. 3(a) & (b) some uniform distribution agglomeration of n-TiC is observed in the Mg and also it is noted that several small nanoparticles are presented. The interface looks in a fine comportment shows the good bonding between the ceramic and matrix. TEM image shows the nano TiC dispersoids embedded homogenously in amorphous phase with the space of 100–200 nm. TEM observation demonstrated that n-TiC particle with average size about 100 nm. Also it is clearly

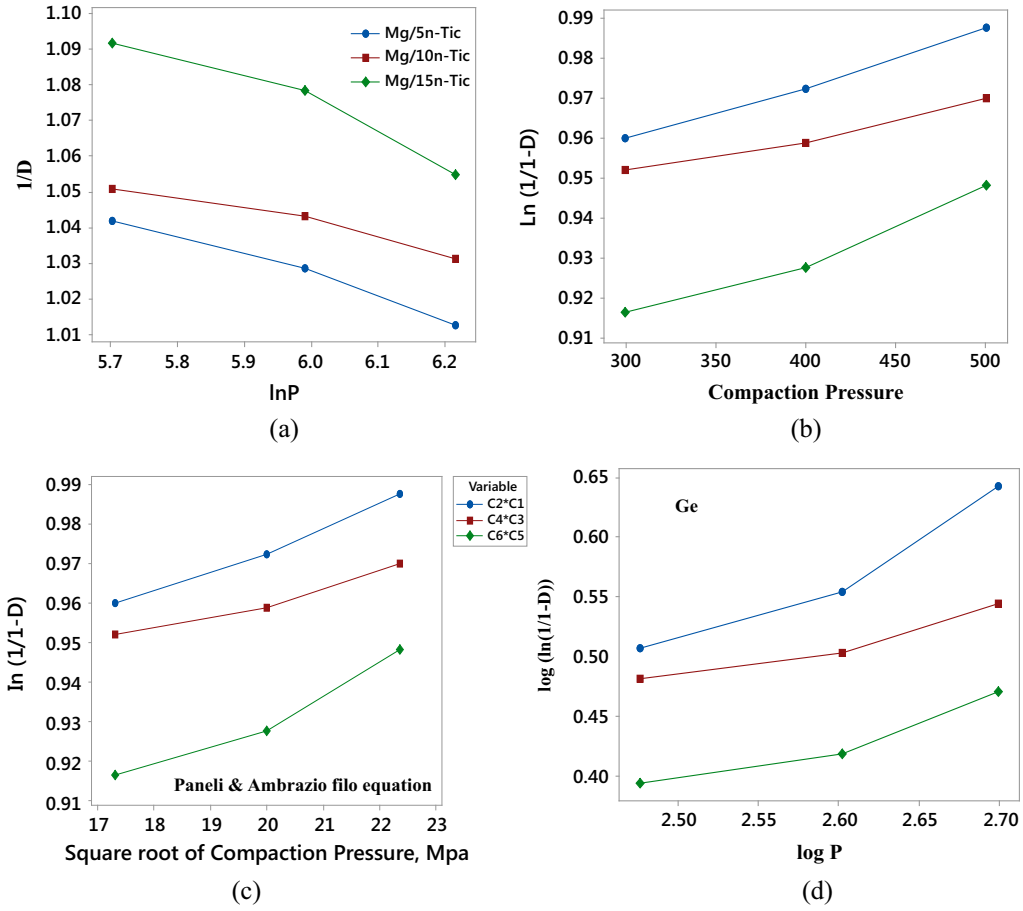

Figure 7 The consolidation behaviour of Mg/5TiC, Mg/10TiC, Mg/15TiC, nanocomposite powders using the (a) Balshin, (b) Heckel, (c) Panelli Ambrosio and Filho, and (d) Ge linear compaction equations.

Table 1 Experimental results for hardness, compressive stress, density and sinterability.

Test number	*A*	*B*	*C*	Green density	Theoretical density	Density	Relative density (%)	Sinterability
1	350	5	300	1.89760	1.79929	1.87460	95.98	0.766044
2	350	10	400	2.05720	1.93790	1.99314	97.22	0.463034
3	350	15	500	2.21681	2.14513	2.17210	98.75	0.376256
4	400	5	400	1.89760	1.80146	1.87898	95.87	0.806324
5	400	10	500	2.05720	1.95412	2.01495	96.98	0.590124
6	400	15	300	2.21680	2.01897	2.12110	95.18	0.516251
7	450	5	500	1.89760	1.78941	1.88747	94.80	0.906369
8	450	10	300	2.05720	1.82285	1.98970	91.61	0.711969
9	450	15	400	2.21680	1.98607	2.14140	92.47	0.673211

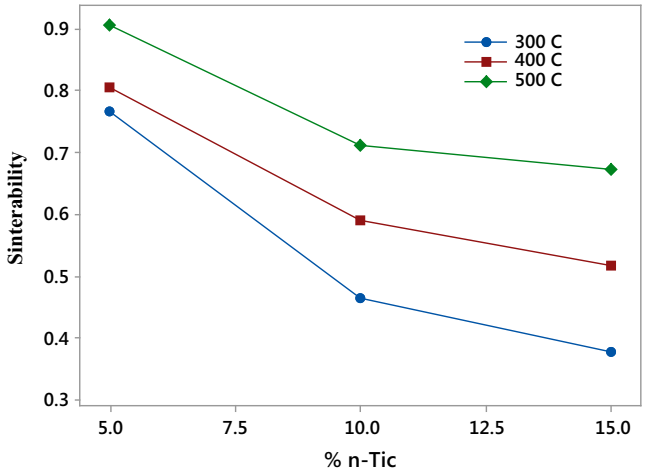

Figure 8 Sinterability curve.

shows that some nanoparticles are present in the composite nearly 60 nm.

The powders are homogeneously mixed at 300 rpm for 1 h. Powders are mixed with a milling medium (Toluene) to prevent oxidation. The homogenized mixed powder with different ratios of TiC is compacted at 400 kN with suitable die. Compacted specimens of Size 10 mm diameter and 25 mm height are examined using Scanning Electron Microscope (SEM). Reinforcement Distribution was examined in the microstructure of the Mg/5 n-TiC, Mg/10 n-TiC, and Mg/15 n-TiC Composite as shown in Fig. 4(a)–(c). It was evident from the microscope image that the reinforcement distribution was quite smooth. The majority of Mg particles consisting of n-TiC is cubic shaped. Mg particles surrounded the n-TiC particles which indicate the good bonding strength. Mg shows the rich zone of the element. It is noted that the laminar shaped Mg particles distributed uniformly around the grain boundary. Besides few micro clusters in the n-TiC, n-TiC is well dispersed in the composite. The well dispersed TiC refines the microstructure of mg and acts as reinforcement of the composite effectively. Obviously no voids are present in the fabricated composite and this indicates the metal is fully dense.

4. EDX mapping

To confirm the elemental presence and avoid the confusion appearance of distinct morphological within the Mg/n-TiC prepared composites materials, EDX mapping will be used. In Fig. 5(a)–(c), microstructure of the composite shows the defect free interface between Mg and n-TiC due to interfacial debonding, EDX analysis observed by SEM confirms the presence of Ti and C, indicating the presence of TiC. The elemental compositions agree with the stoichiometric relations of the prepared compound. The EDX peak of Mg is bigger than the average n-TiC. No oxygen peaks were observed in the matrix area, validating that the fabricated composite free from additional contamination from the atmosphere. Black regions present in the mapping images are distracted province due to surface irregularities and therefore no element was identified.

5. Densification, compressibility, sinterability behaviour of nanocomposites

The compaction of nanocomposite powders has recently garnered interest [20], as it decides the densification of bulk materials. In general, the density positively correlated with the compaction pressure at decelerating rates during cold uniaxial pressing or compaction. The consolidation of various metal and ceramic powders during die compaction has been previously studied by researchers [32–35]. Generally, consolidation involves two main stages: particle sliding/rearrangement and plastic deformation [36]. The particle sliding/rearrangement mechanism dominates at low compaction pressures, and the plastic deformation mechanism dominates at high compaction pressures. The addition of hard ceramic particles was found to decrease the densification rate [37]. In this study, the range of pressure was taken as 300 MPa, 400 MPa, 500 MPa, the density was measured and the compressibility curves were drawn for Mg/5 n-TiC, Mg/10 TiC, and Mg/15 n-TiC nanocomposites. The compressibility curves are shown in Fig. 6.

From this study, the Mg/5 TiC nanocomposite exhibited excellent densification behaviour for the same range of compaction pressures when compared to the Mg/10 n-TiC and Mg/15 n-TiC nanocomposite powders. This effect was attributed to the Content of n-TiC. Due to the addition of n-TiC to the Mg matrix, the particle rearrangement was significant due to the disintegration of the clusters and agglomerates under the applied load and the filling of the voids between the matrix particles. However, the amount of plastic deformation was low due to the load partitioning effect [37,38].

Fig. 7 shows the evaluation of the consolidation behaviour of Mg/5 n-TiC, Mg/10 n-TiC, and Mg/15 n-TiC, nanocomposite powders using the Balshin, Heckel, Panelli Ambrosio and

Table 2 The fitting constant (K) and correlation coefficient (R^2) values of the Mg/TiC nanocomposites using various compaction equations.

Temperature	% TiC	Pressure	Balshin		Heckel		Panelli		Ge	
			K, Mpa^{-1}	R^2	K, Mpa^{-1}	R^2	K, Mpa^{-1}	R^2	K, Mpa^{-1}	R^2
350	5	300	0.132795	0.0151392	0.0044665	0.0012142	0.0773626	0.0118132	0.552043	0.0215753
350	10	400	0.151782	0.0019588	0.0039816	0.0001608	0.0796321	0.0009865	0.552853	0.0006657
350	15	500	0.182241	0.0213709	0.0044332	0.0000856	0.0991289	0.0044018	0.566796	0.0379598
400	5	400	0.126585	0.0208449	0.0032724	0.0000695	0.0654489	0.0010379	0.528607	0.0467590
400	10	500	0.148520	0.0040679	0.0029707	0.0007373	0.0664259	0.0096190	0.544966	0.0125439
400	15	300	0.169779	0.0255625	0.0030411	0.0001527	0.0526736	0.0044902	0.661722	0.0752328
450	5	500	0.118207	0.0242372	0.0021399	0.0005750	0.0478486	0.0053165	0.524852	0.0677744
450	10	300	0.128216	0.0006406	0.0016298	0.0003707	0.0282291	0.0086011	0.644089	0.0000112
450	15	400	0.151526	0.0186742	0.0012056	0.0005700	0.0241129	0.0074149	0.661973	0.0361367

Filho, and Ge linear compaction equations. Table 2 summarizes the densification coefficient (K) and correlation coefficient (R^2) for the above linear equations. Table 2 shows that the Mg/n-TiC powder had the highest K-value, which indicates its higher plastic deformation capacity due to a more ductile nature and irregular morphology.

The densification rate of the Mg/n-TiC powder was lower than that of the microcrystalline powder due to the work-hardening effect. The addition of n-TiC reinforcement decreased the densification (K-value) rate, and the plastic deformation capacity of composite powders was significantly reduced by the MA. The powder density always depends on

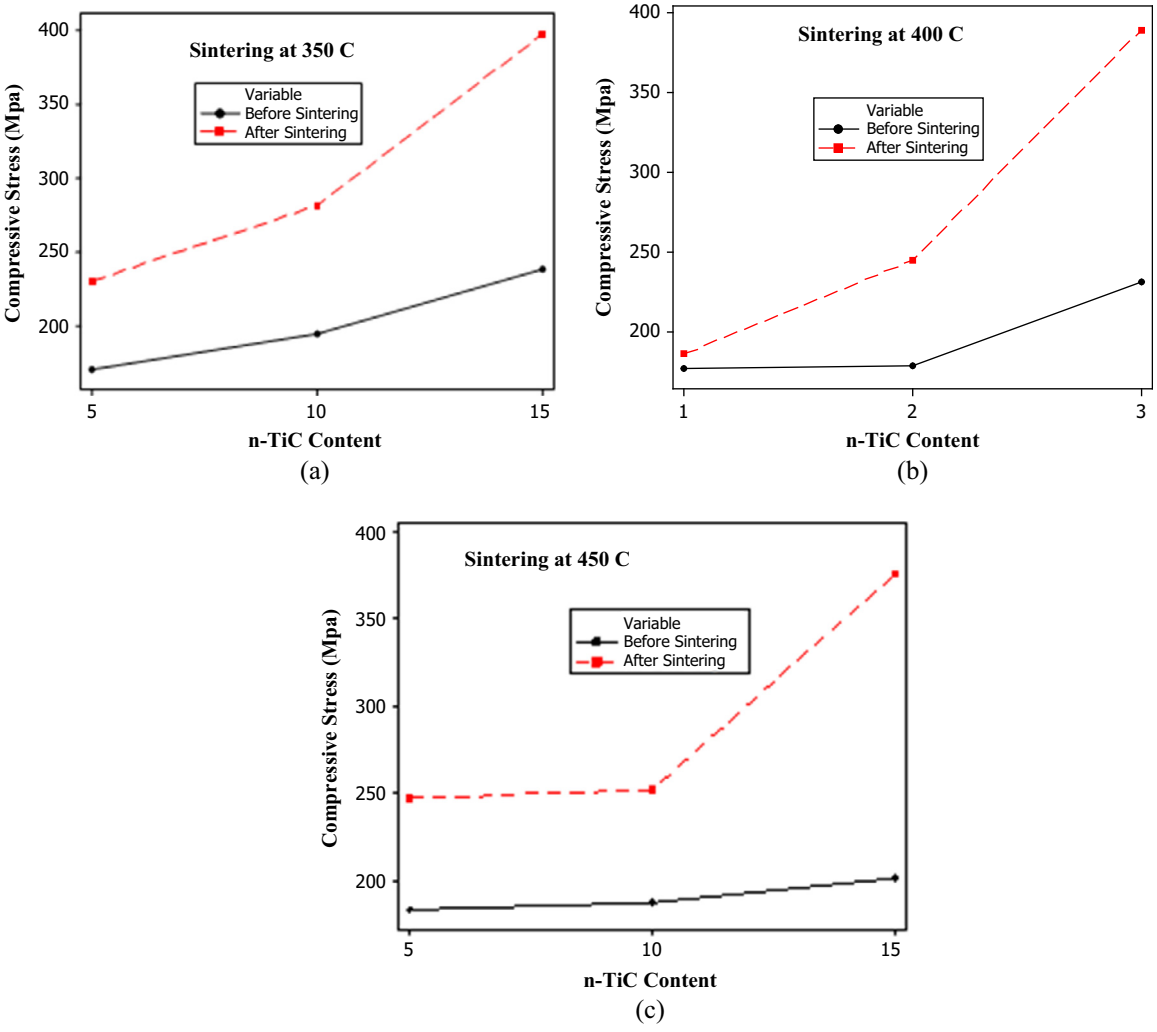

Figure 9 Compressive stress with respect to n-TiC content at different Sintering Temperatures (a) 300 °C (b) 400 °C (c) 500 °C.

Table 3 Result for compressive stress before sintering and after sintering.

Test number	Compressive load (MPa)	n-Tic content	UCS (before Sintering)	Sintering temperature (°C)	UCS (after Sintering)
1	350	5	170	300	230
2	350	10	179	400	245
3	350	15	187	500	252
4	400	5	177	400	186
5	400	10	183	500	247
6	400	15	194	300	281
7	450	5	201	500	376
8	450	10	238	300	397
9	450	15	231	400	389

the size, morphology and size distribution of the particles [35,37].

Table 1 shows the densities of Mg for various n-TiC contents (wt%) at 350 °C, 400 °C, and 450 °C. The density initiates to be positively linked to the sintering temperature from 350 °C to 450 °C. The sinterability of the compacted materials was evaluated by using the following equation [39]:

$$\varphi = \frac{\rho s - \rho g}{\rho th - \rho g}$$

where ρs, ρg and ρth are the sintered, green and theoretical densities, respectively. Fig. 8 shows the sinterability of the compacted materials as a function of the wt% of n-TiC reinforcement.

The sinterability of nanocomposites decreased for a increasing content of the n-TiC nanoparticles from 5 to 15 wt%, due to the morphology of the milled powder. The sinterability was found to be positively correlated with the sintering temperatures (350–450 °C). The decrease in the sinterability was very high at 450 °C compared to the sinterability at both 350 °C and 400 °C. The compaction characteristic curves for the Mg/n-TiC nanocomposite powders are presented in Fig. 8. In general, the curves indicate the typical powder compressibility behaviour of metallic powders, i.e. the density increases with increasing compaction pressure at a decelerating rate. It is important to note that the densification behaviour was influenced by the powder characteristics and the method of processing.

In general, the density was positively correlated with the compaction pressure at decelerating rates during cold uniaxial pressing or compaction. The compaction behaviour of Mg/n-TiC powders was also observed for comparison purposes. In this study, the Mg/n-TiC exhibited excellent densification behaviour for the various ranges of compaction pressures (see Fig. 9).

6. Compressive strength examination

In order to find out the compression strength of the Mg/n-TiC composite, the experiment was carried out using flat faced dies and a hydraulic operated universal compression testing machine of having 1 MN capacity. The testing was carried out on room temperature. The compressive strength of metal matrix composite depends not only on the mechanical properties of the metal matrix and the ceramic particles but also on the volume fraction, structure and distribution of the ceramic particles. The interfacial bonding between the metal matrix and the ceramic particles and the amount of defects in the composite also affect the compressive strength. Table 3 shows the ultimate compression stress of the composites before sintering and after sintering.

It is inferred that with the addition of n-TiC and also with sintering temperature, the compressive stress and hardness were increased. Overall, compressive strength of the composite material is higher than that of the unreinforced Pure Mg. Further, it is observed that increase in compressive strength, with an increase in n-TiC reinforcement, is much higher when compared to the strength improvement observed in some other magnesium matrix composite.

7. Conclusion

- The powder metallurgy method is one of the effective methods and easy process to disperse the nano TiC in the Magnesium matrix.
- Elemental mixing was effective for providing uniformly mixed powder and resulted in uniform dispersion of TiC in the Pure Mg.
- Due to the presence of TiC, the morphology of the Mg phase is changed to discontinuous and fine. Results of EDX-analysis indicate the absence of oxide and silicide phase at Mg/TiC interface.
- The improvement of mechanical properties of composites is attributed to the grain refinement and the strengthening effects caused by the Nano TiC. The stress value is increased with respective to the addition of TiC and Compaction Pressure.
- The sinterability was decreased with an increasing weight percentage of n-TiC. The compressibility curves were obtained using the Balshin, Heckel, Panelli, Ambrozio Filho and Ge equations.
- The addition of a hard ceramic reinforcement decreased the densification coefficient (K).
- Thee compressibility behaviour of powders in terms of particle rearrangement and plastic deformation mechanisms was investigated. The compaction data were best fitted to the Panelli, Heckel, Ambrozio Filho and Ge equation in order to consider the effect of applied pressure.

References

[1] M. Habibnejad-Korayem, R. Mahmudi, W.J. Poole, Mater. Sci. Eng. A 519 (2009) 198–203.
[2] C. Blawert, N. Hort, K.U. Kainer, Trans. Indian Inst. Met. 57 (2004) 397–408.
[3] K.F. Farraro, K.E. Kim, S.L. Woo, J.R. Flowers, M.B. McCullough, J. Biomech. 47 (2014) 1979–1986.

[4] B. Zberg, P.J. Uggowitzer, J.F. Löffler, Nat. Mater. 8 (2009) 887–891.
[5] Y. Song, D. Shan, R. Chen, F. Zhang, E.H. Han, Mater. Sci. Eng. C 29 (2009) 1039–1045.
[6] S.M. Masoudpanah, R. Mahmudi, Mater. Sci. Eng. A 526 (2009) 22–30.
[7] Abhilash Viswanath, H. Dieringa, K.K. Ajith Kumar, U.T.S. Pillai, B.C. Pai, Investigation on mechanical properties and creep behavior of stir cast AZ91-SiCp composites, J. Magnesium Alloys (Available online 5 March 2015).
[8] H. Dieringa, Properties of magnesium alloys reinforced with nanoparticles and carbon nanotubes: a review, J. Mater. Sci. 46 (2011) 289–306.
[9] S.C. Tjong, Novel nanoparticle reinforced metal matrix composites with enhanced mechanical properties, Adv. Eng. Mater. 9 (2007) 639–652.
[10] S.F. Hassan, M. Gupta, Development of high performance Mg nanocomposites using nano-Al_2O_3 as reinforcement, Mater. Sci. Eng. A 392 (2005) 163–168.
[11] B.W. Chua, L. Lu, M.O. Lai, Compos. Struct. 47 (1999) 595–601.
[12] J. Hashim, L. Looney, M.S.J. Hashmi, J. Mater. Process. Technol. 92–93 (1999) 1–7.
[13] B. Winkler, E.A. Juarez-Arellano, A. Friedrich, L. Bayarjargal, J. Yan, S.M. Clark, J. Alloy. Compd. 478 (2009) 392–397.
[14] G. Wen, S.B. Li, B.S. Zhang, Z.X. Guo, Reaction synthesis of TiB_2-TiC composites with enhanced toughness, Acta Mater. 49 (8) (2001) 1463–1470.
[15] X. Tao, J. Du, Y. Yang, Y. Li, Y. Xia, Y. Gan, H. Huang, W. Zhang, X. Li, Cryst. Growth Des. 11 (2011) 4422–4426.
[16] W.J. Li, R. Tu, T. Goto, Preparation of directionally solidified TiB_2-TiC eutectic composites by a floating zone method, Mater. Lett. 60 (6) (2006) 839–843.
[17] A. Contreras, C.A. León, R.A.L. Drew, E. Bedolla, Wettability and spreading kinetics of Al and Mg on TiC, Scripta Mater. 48 (12) (2003) 1625–1630.
[18] A. Contreras, A. Albiter, R. Pérez, Microstructural properties of the Al-Mg/TiC composites obtained by infiltration techniques, J. Phys.: Condens. Matter 16 (22) (2004) S2241–S2249.
[19] J. Laloy, O. Lozano, L. Alpan, J. Mejia, O. Toussaint, B. Masereel, J.-M. Dogné, S. Lucas, Toxicol. Rep. 1 (2014) 172–187.
[20] Z. Razavi Hesabi, H.R. Hafizpour, A. Simchi, An investigation on the compressibility of aluminum/nano-alumina composite powder prepared by blending and mechanical milling, Mater. Sci. Eng. A 454/455 (2007) 89–98.
[21] R.M. German, Powder Packing Characteristics, Metal Powder Industries Federation, pp. 220–223.
[22] P.J. Denny, Compaction equations: a comparison of the Heckel and Kawakita equations, Powder Technol. 127 (2002) 162–172.
[23] R. Panelli, Francisco Ambrozio Filho, A study of a new phenomenological compacting equation, Powder Technol. 114 (2001) 255–261.
[24] R. Ge, A new powder compaction equation, Int. J. Powder Metall. 27 (1991) 211–216.
[25] H.R. Hafizpour, A. Simchi, S. Parvizi, Analysis of the compaction behavior of Al–SiC nanocomposites using linear and non-linear compaction equations, Adv. Powder Technol. 21 (2010) 273–278.
[26] Keke Gan, Mingyuan Gu, The compressibility of Cu/SiCp powder prepared by high-energy ball milling, J. Mater. Process. Technol. 199 (2008) 173–177.
[27] S. Hwang, C. Nishimura, P. McCormick, Scripta Mater. 44 (2001) 2457–2462.
[28] D. Jeyasimman, S. Sivasankaran, K. Sivaprasad, R. Narayanasamy, R.S. Kambali, An investigation of the synthesis, consolidation and mechanical behaviour of Al 6061 nanocomposites reinforced by TiC via mechanical alloying, Mater. Des. 57 (2014) 394–404.
[29] M. Eckert, Disputed discovery: the beginnings of X-Ray diffraction in crystals in 1912 and its repercussions, Acta Crystallogr. Sect. A 68 (2012) 30–39.
[30] H.M. Rietveld, Acta Crystallogr. A228 (1966) 21.
[31] J. Rodriguez-Carvajal, Collected Abstract of Powder Diffraction Meeting, in: J. Galy Toulouse (Ed.), France, 1990, p. 127.
[32] C. Suryanarayana, Mechanical alloying and milling, Prog. Mater Sci. 46 (2001) 1–184.
[33] C. Kursun, M. Gogebakan, Characterization of nanostructured Mg–Cu–Ni powders prepared by mechanical alloying, J. Alloy. Compd. 619 (2015) 138–144.
[34] M. Gogebakan, C. Kursun, J. Eckert, Formation of new Cu-based nanocrystalline powders by mechanical alloying technique, Powder Technol. 247 (2013) 172–177.
[35] H.R. Hafizpour, A. Simichi, S. Parvizi, Analysis of the compaction behaviour of Al–SiC nanocomposites using linear and non-linear compaction equations, Adv. Powder Technol. 21 (2010) 273–278.
[36] S. Sivasankaran, K. Sivaprasad, R. Narayanasamy, Vijay Kumar Iyer, An investigation on flowability and compressibility of AA 6061_{100-x}-x wt.% TiO_2 micro and nanocomposite powder prepared by blending and mechanical alloying, Powder Technol. 201 (2010) 70–82.
[37] Keke Gan, Mingyuan Gu, The compressibility of Cu/SiCp powder prepared by high energy ball milling, J. Mater. Process. Technol. 62 (2008) 282–285.
[38] Z. Razavi Hesabi, H.R. Hafizpour, A. Simichi, An investigation on compressibility of aluminum/nano-alumina composite powder prepared by blending and mechanical milling, Mater. Sci. Eng. A 454–455 (2007) 89–98.
[39] D. Jeyasimman, S. Sivasankaran, K. Sivaprasad, R. Narayanasamy, R.S. Kambali, An investigation of synthesis, consolidation and mechanical behaviour of Al 6061 nanocomposites reinforced by TiC via mechanical alloying, Mater. Des. 57 (2014) 394–404.